JOURNAL OF AGRICULTURAL AND FOOD CHEMISTRY

pubs.acs.org/JAFC Article

Curcumin−Cu(II) Ensemble-Based Fluorescence "Turn-On" Mode Sensing the Plant Defensive Hormone Salicylic Acid *In Situ* and *In Vivo*

Chong Chen,[#] Lin-Lin Yang,[#] A-Ling Tang, Pei-Yi Wang,* Rong Dong, Zhi-Bing Wu, Zhong Li, and Song Yang*

Cite This: https://dx.doi.org/10.1021/acs.jafc.0c01283 Read Online

ACCESS | Metrics & More | Article Recommendations | Supporting Information

ABSTRACT: Salicylic acid (SA), a crucial, plant-derived signal molecule, is capable of launching global transcriptional reprogramming to assist plants in obtaining the systemic acquired resistance (SAR) mechanism. Thus, the accurate detection of SA will not only significantly contribute to the understanding of the plant SAR but also contribute to crop protection and to the security of the agricultural production and food supply. However, detection of SA using fluorescent probes is a great challenge for scientists, because SA analogues can significantly interfere with the detection results. Herein, we first reported using a simple, natural curcumin−Cu^{2+} ensemble to selectively and sensitively monitor SA *in situ* and *in vivo*, directed by a fluorescence "turn-on" mode. A binary combination curcumin−Cu^{2+} was first fabricated with a fluorescence "turn-off" pattern caused by the paramagnetic nature of Cu^{2+}. Subsequently, a fluorescence "turn-on" response was performed for detecting SA accompanied by the formation of the ternary complex curcumin−Cu^{2+}−SA due to the high affinity of SA toward Cu^{2+}, which reduced the fluorescent impact caused by the paramagnetism of Cu^{2+}. Further study revealed that the rationally designed hybrid probe could monitor SA in living cell lines. We anticipate that this finding can inspire the discovery of a high-performance SA probe.

KEYWORDS: *curcumin−Cu^{2+} ensemble, selective detection, salicylic acid, fluorescence "turn-on"*

1. INTRODUCTION

Salicylic acid (SA) is one of the significant biogenic immune signals and regulators existing widely in the plant kingdom.[1−3] It is capable of launching global transcriptional reprogramming to motivate plants to systemically express a type of resistant, pathogenesis-related species, which is dedicated to resistance.[4,5] Through this process, plants can be conferred with persistent protection abilities against incompatible pathogens, which is called systemic acquired resistance (SAR).[6−8] Generally, SA is generated from the infected tissue and accumulates in the systemic, uninfected tissue after an invasion of various offensive pathogens, including viruses, fungi, bacteria, and oomycetes.[9,10] Also, many studies have demonstrated that SA-induced signal pathways can be dramatically regulated by the amount of endogenic SA.[10,11] Thereby, the accurate detection of SA can elucidate the SA-induced SAR mechanism, which will significantly help the staple crops obtain defense mechanisms against various pathogen infections. Simultaneously, this action may also initiate the discovery of novel immune activators that offer a new approach that can reduce the use of traditionally harmful pesticides, whose use concerns people who handle crop protection. However, SA analogues, such as methyl salicylate, 2-methoxybenzoic acid, *m*-hydroxybenzoic acid, *o*-toluic acid, benzoic acid, *p*-hydroxybenzoic acid, and catechol, can significantly interfere with the detection results, which makes the detection of SA a big challenge.[12−15] Therefore, the development of simple, reliable, and accurate techniques to detect the biological signaling molecule SA *in situ* and *in vivo* is in great demand.

In the past decades, various detection strategies have been developed to monitor SA, for instance, HPLC,[16−19] gas chromatography,[20,21] colorimetry,[22] spectrofluorimetry,[23−25] surface plasma resonance technology,[26] and electrochemical analysis.[27,28] However, these methods had drawbacks, including expensive instruments, low selectivity, complicated sample preparation procedures, and time-consuming sample testing processes. As far as we know, using the above-mentioned methods cannot achieve the goal of real-time detection of SA in living organisms.

Fluorescence probes offer encouraging opportunities and promising applications in detecting SA in terms of their privileged characteristics, including good sensibility and selectivity,[29,30] fast response,[31−33] low detection limits,[34,35] and real-time monitoring.[36,37] In particular, metal-based fluorescent ensembles have been extensively studied and developed for monitoring signal species on account of their convenient synthetic procedures, improved water solubilities, multifunctional testing purposes, and perceptible detection

Received: February 24, 2020
Revised: April 7, 2020
Accepted: April 10, 2020

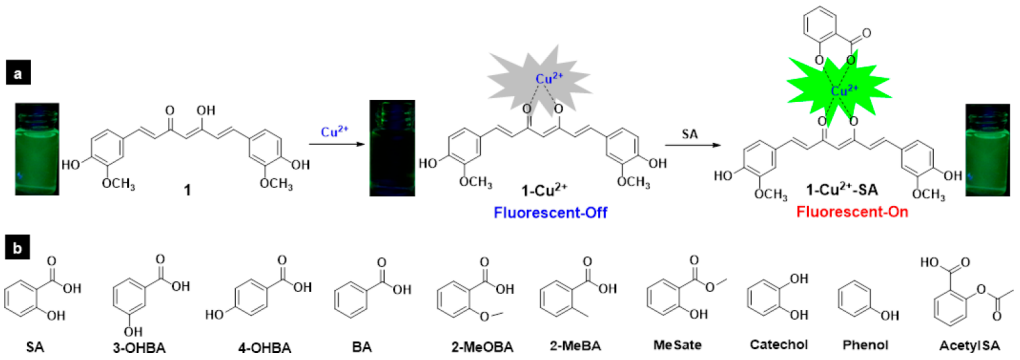

Figure 1. (a) Proposed mechanisms for detecting SA via the **1**−Cu^{2+} ensemble. (b) Structures for SA and SA analogues.

mechanism.[38] Curcumin (1,7-bis(4-hydroxy-3-methoxyphenyl)-1,6-heptadiene-3,5-dione, **1**), found in the rhizomes of *Curcuma longa* Linn., not only is an important, bioactive, naturally occurring product but also is recognized as a promising fluorescent probe that possesses rich photophysical and photochemical properties due to the unsaturated *β*-diketone moiety in which it can induce a keto−enol tautomerism. Numerous studies revealed that the pattern of the 1,3-diketones scaffold can incorporate metals to form complexes which have already exerted reasonable applications in photochemistry and photobiology.[39−41] Herein, curcumin−metal complexes were rationally fabricated to monitor SA *in situ* and *in vivo*. As far as we know, no report was performed via exploiting a curcumin−metal-based fluorescent sensor for selectively and sensitively sensing SA with a naked-eye detection feature. Moreover, a plausible detection mechanism was recommended (Figure 1a): Preliminarily, Cu^{2+} was selected and employed to bind the *β*-diketone part of curcumin to form the **1**−Cu^{2+} ensemble, which resulted in the fluorescent "turn-off" of curcumin because of the paramagnetic nature of Cu^{2+}. SA was added into the system; subsequently, this led to the formation of the ternary complex **1**−Cu^{2+}−SA, which was accompanied by the fluorescence "turn-on" due to SA having a high affinity toward Cu^{2+}.[42−44] Thus, the fluorescent impact caused by the paramagnetism of Cu^{2+} was reduced. As indicated, the fluorescence of **1** was observed to be quenched immediately after adding Cu^{2+}, which, subsequently, was recovered along with the addition of SA, indicating that a colorimetric sensor for naked-eye monitoring SA should be discovered.

2. MATERIALS AND METHODS

2.1. Instruments. NMR data were recorded by JEOL-ECX-500 devices (tetramethylsilane was the internal standard, deuterated dimethyl sulfoxide (DMSO-d_6) or chloroform ($CDCl_3$) was the solvent). High-resolution mass spectra were recorded by Agilent LC/MSD Trap VL and Thermo Scientific Q Exactive mass spectrometers. Fluorescence spectra were measured by a Fluoromax-4 (Horiba LTD). Cell imaging was carried out by an Olympus FVMPE-RS multiphoton confocal laser scanning microscope.

2.2. Chemicals. The used chemical reagents, including *N*,*N*-dimethylformamide (DMF), ethyl acetate (EtOAc), petroleum ether, and dichloromethane, were acquired from reliable suppliers without additional treatment. Deionized water was exploited in all of the experiments. All of the metallic compounds were composed of nitrate ions. Potassium carbonate (K_2CO_3), ammonium chloride, iodomethane, boron oxide, acetylacetone, 3,4-dihydroxybenzaldehyde, tributyl borate, and butylamine were purchased from Aladdin Reagent (Shanghai) Co., Ltd. Curcumin (purity >98%) was purchased from Energy Chemical of Saen Chemical Technology (Shanghai) Co., Ltd., and the additionally purified curcumin product was obtained by recrystallization in ethanol.

2.3. Procedures for Fluorescence Spectral Studies. The initial solution of all of the probes and metal ions was configured as 1.0 mM in DMF/H_2O (7:3, v/v) and deionized water, respectively. The stock solution (1.0 mM) of the **1**−Cu^{2+} ensemble was obtained by blending probe **1** with the same amount of Cu^{2+} in DMF/H_2O (7:3, v/v). The stock solution (1.0 mM) of other ensembles, such as **2**−Cu^{2+}, **3**−Cu^{2+}, and **4**−Cu^{2+}, followed the above procedure. The stock solutions (1.0 mM) of SA and its analogues were prepared in DMF/H_2O (7:3). Sample preparation for the fluorescence testing is described in the following: A certain amount of detected objects was added to a volumetric bottle containing 0.1 mL of probes (1.0 mM). Then, the mixed solution was fixed to 10 mL with the same solvent before testing.

2.4. Synthetic Protocols for Compounds 2, 3, and 4. *2.4.1. Synthesis of Compound 2.* Curcumin (**1**, 200 mg, 0.54 mmol) and K_2CO_3 (38 mg, 0.27 mmol) were dissolved in 5 mL of dry DMF, and the mixture was cooled with an ice bath. Then, iodomethane (39 mg, 0.27 mmol) in 1 mL of dry DMF was added dropwise, and the obtained solution was magnetically stirred for about 30 min. After that, 40 mL of EtOAc was added, and the organic layer was washed by a saturated ammonium chloride solution. A crude product was provided by vacuum distillation. Finally, the pure compound **2** was afforded by using a common column chromatography with mixed petroleum ether and EtOAc solvents. Yield 34.7%. ^{1}H NMR (500 MHz, $CDCl_3$, *δ*): 7.58 (dd, 2H, *J* = 7.5 Hz, −CH═), 7.12 (dd, 2H, *J* = 10.0 Hz, Ar−H), 7.07 (s, 2H, Ar−H), 6.89 (dd, 2H, *J* = 10.0 Hz, ═CH−), 6.47 (dd, 2H, *J* = 10.0 Hz, Ar−H), 5.91 (s, 1H, −CH═), 5.80 (s, 1H, −OH), 3.93 (s, 6H, $-OCH_3$), 3.92 (s, 3H, $-OCH_3$). ^{13}C NMR (125 MHz, $CDCl_3$, *δ*): 183.5, 183.2, 151.1, 149.3, 147.9, 146.9, 140.7, 140.5, 128.1, 127.7, 123.0, 122.7, 122.1, 121.8, 114.9, 111.2, 109.8, 109.7, 101.3, 56.1, 56.0, 55.9. HRMS (ESI): $[M - H]^-$ calcd for $C_{22}H_{21}O_6$, 381.1344; found, 381.1342.

2.4.2. Synthesis of Compound 3. The synthesis of **3** followed the protocol of compound **2**. The difference is that the dosages of K_2CO_3 and iodomethane were changed to 150 mg (1.08 mmol) and 153 mg (1.08 mmol), respectively. Yield 75.3%. ^{1}H NMR (500 MHz, $CDCl_3$, *δ*): 7.69 (d, 2H, *J* = 15.0 Hz, −CH═), 7.19 (dd, 2H, *J* = 10.0 Hz, Ar−H), 7.10 (s, 2H, Ar−H,), 6.98 (d, 2H, *J* = 15.0 Hz, ═CH−), 6.89 (dd, 2H, *J* = 10.0 Hz, Ar−H), 6.51 (s, 1H, −CH═), 3.95 (s, 12H, $-OCH_3$). ^{13}C NMR (125 MHz, $CDCl_3$, *δ*): 182.6, 151.0, 149.3, 141.4, 128.6, 122.6, 118.8, 111.2, 110.2, 105.8, 56.1, 56.0. HRMS (ESI): $[M - H]^-$ calcd for $C_{23}H_{23}O_6$, 395.1500; found, 395.1504.

2.4.3. Synthesis of Compound 4. The synthetic protocol followed the literature procedure reported by Sharma et al.[45] Boron oxide (0.49 g, 7.0 mmol) and acetylacetone were dissolved in ethyl acetate (10 mL) and stirred for 30 min in a 45 °C oil bath. Then, 3,4-dihydroxybenzaldehyde (2.76 g, 20.0 mmol) and tributyl borate (0.46 g, 20.0 mmol) were added, and the obtained solution was magnetically stirred for about 30 min. Later, butylamine (1.10 g, 15.0 mmol), in 10 mL of ethyl acetate, was added dropise. The obtained mixture was stirred for anothor 24 h. Subsequently, 10 mL of 10% hydrochloric acid was added and incubated at 60 °C for 1 h.

https://dx.doi.org/10.1021/acs.jafc.0c01283
J. Agric. Food Chem. XXXX, XXX, XXX−XXX

Finally, the organic layer was obtained by simple separation and was evaporated under reduced pressure to give the crude product. The pure compound **4** was provided by using column chromatography with the mixed eluting agents of dichloromethane and EtOAc. Yield 1.3%. ^{1}H NMR (500 MHz, DMSO-d_6, δ): 9.60 (s, 2H), 9.15 (s, 2H), 7.46 (d, J = 15.0 Hz, 2H), 7.01 (d, J = 10.0 Hz, 2H), 6.78 (d, J = 10.0 Hz, 2H), 6.57 (d, J = 15.0 Hz, 2H), 6.07 (s, 2H). ^{13}C NMR (125 MHz, DMSO-d_6, δ): 183.1, 148.4, 145.6, 140.7, 126.3, 121.5, 120.6, 115.8, 114.7, 100.9. HRMS (ESI): $[M - H]^-$ calcd for $C_{19}H_{15}O_6$, 339.0874; found, 339.0874.

3. RESULTS AND DISCUSSION

3.1. Preparation of Nonfluorescent Curcumin−Cu^{2+} Ensemble. In order to prepare the fluorescent "turn-off" curcumin−metal ensemble, various metal ions were screened by using fluorescence spectroscopy. As illustrated in Figure 2a,

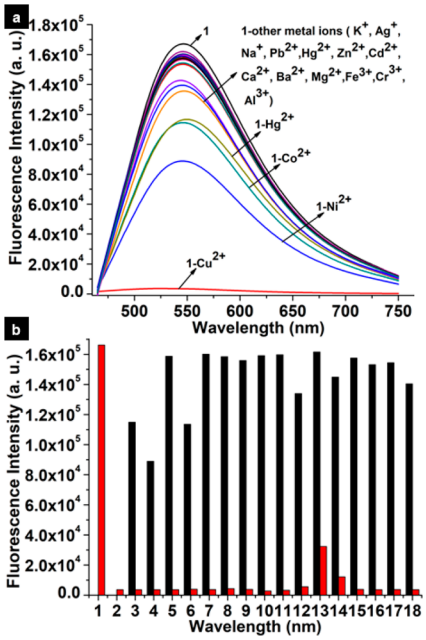

Figure 2. (a) Fluorescent spectra of **1** (10 μM) toward 1 equiv of various cations. (b) Competition experiments for adding Cu^{2+} (red bars, 1 equiv, 3−18) into the premixed solution consisting of probe **1** (10 μM) and various interfering metal ions (blank bars, 2 equiv, 3−18): (1) probe **1** itself, (2) probe **1** + Cu^{2+}, (3) Co^{2+}, (4) Ni^{2+}, (5) Pb^{2+}, (6) Hg^{2+}, (7) Zn^{2+}, (8) Cd^{2+}, (9) Ca^{2+}, (10) Ba^{2+}, (11) Mg^{2+}, (12) Fe^{3+}, (13) Cr^{3+}, (14) Al^{3+}, (15) Li^+, (16) K^+, (17) Na^+, and (18) Ag^+. Conditions: DMF/H_2O (7:3, v/v), $\lambda_{ex}/\lambda_{em}$ = 433/530 nm, slits = 3 nm/3 nm.

Cu^{2+} can not only quench the fluorescence of **1** within 10 s (Figure S1) but also be selectively distinguished in comparison to other metal ions, indicating that the natural, fluorescent curcumin can detect Cu^{2+} with a high specificity. Competition experiments were further conducted to explore the selectivity of **1** toward Cu^{2+} by testing the variations of the fluorescent intensity before and after the addition of Cu^{2+} into the premixed ingredients that contained **1** with other metal ions. The fact that the fluorescence can be significantly quenched only by the later introduction of Cu^{2+} further supports that excellent anti-interference performance is achieved by probe **1** in the detection of Cu^{2+} (Figure 2b). The Job's plot experiment revealed that a 1:1 stoichiometry was provided for probe **1** and Cu^{2+} with the binding constant of 5.54×10^4 M^{-1} (Figures S2 and S3), which was in accordance with the result from HRMS, affording the peak at m/z 430.0473 that corresponds to [**1**−Cu^{2+}] (Figure S4). Further study revealed that the related detection limit of probe **1** toward Cu^{2+} was 15 nM. Based on the above results, the curcumin−Cu^{2+} ensemble was successfully constructed, in which curcumin exerted a high specificity and sensitivity toward Cu^{2+} with a fluorescent "turn-off" mode.

3.2. Selective Detection of SA by the Curcumin−Cu^{2+} Ensemble. The prepared **1**−Cu^{2+} was employed to examine the selectivity for SA analogues by using fluorescence microscopy and UV light. Before the detection of SA, the solvent was first screened. As shown in Figure S5a, the **1**−Cu^{2+} ensemble displayed the highest response to SA in DMF solvent, providing a 26-fold enhancement in the fluorescence intensity (Figure S5b). To extend its potential applications, the solvent water was introduced into the system. However, along with the increase in the ratio of water, the fluorescence intensity of **1**−Cu^{2+}−SA was significantly decreased (Figure S5c). Because of this, the solution of DMF/H_2O with the volume ratio 7:3 afforded the better response (20.6-fold enhancement) for detecting SA (Figure S5d). Based on the above results, the detection of SA by the **1**−Cu^{2+} ensemble was performed in the DMF/H_2O (7:3, v/v) solution. Clearly, a remarkable, induced fluorescence "turn-on" pattern (Figure 3a) was observed only upon the addition of SA within 10 s (Figure S6). This occurrence simultaneously promoted the variation of fluorescence quantum yields from 0.002 (**1**−Cu^{2+}) to 0.025 (**1**−Cu^{2+}−SA). The presented green fluorescence under the UV light (Figure 3b) further confirmed that the **1**−Cu^{2+} binary complex possessed the specific selectivity and sensitivity in response to SA compared to those of other SA analogues, including 4-hydroxybenzoic acid (4-OHBA), 3-hydroxybenzoic acid (3-OHBA), benzoic acid (BA), 2-methoxybenzoic acid (2-MeOBA), 2-methylbenzoic acid (2-MeBA), methyl salicylate (MeSate), catechol, phenol, acetylsalicylic acid (AcetylSA), anthranilic acid, and 5-aminosalicylic acid (Figure S7). Moreover, the **1**−Cu^{2+} ensemble could selectively distinguish SA in MES buffer (4-morpholineethanesulfonic acid; 20 mM; DMF/MES buffer = 7/3 or 5:5, v/v; pH 7.2) from pyrophosphate and adenosine triphosphate (Figure S8). Additionally, the **1**−Cu^{2+} ensemble could monitor SA in a wide pH range in DMF/MES buffer; however, the better detection system was in a neutral or weakly basic solution (Figure S9). Competition experiments were further performed to evaluate the anti-interference performance of the **1**−Cu^{2+} ensemble toward SA via the addition of SA into the premixed solution containing **1**−Cu^{2+} with other SA analogues. Dramatically, the significantly increased fluorescent intensity could be achieved due to the latter addition of SA (Figure 3c), further confirming that the **1**−Cu^{2+} ensemble can be exploited as a highly selective sensor for monitoring SA with an attractive anti-interference feature. The titration experiment of the **1**−Cu^{2+} ensemble toward SA demonstrated that the fluorescent intensity at 530 nm was gradually elevated with increments of SA and was afforded the binding constant of 5.22×10^4 M^{-1} (Figure S10a−c). Therefore, an appreciable linear detection range was obtained from 10 to 150 μM (Figure S10d). Further study revealed that the related detection limit of the **1**−Cu^{2+} ensemble toward SA was 3 μM. Given the above results, the rationally designed **1**−Cu^{2+} complex can be considered as a promising colorimetric probe for sensing SA with the appreciable feature.

https://dx.doi.org/10.1021/acs.jafc.0c01283
J. Agric. Food Chem. XXXX, XXX, XXX−XXX

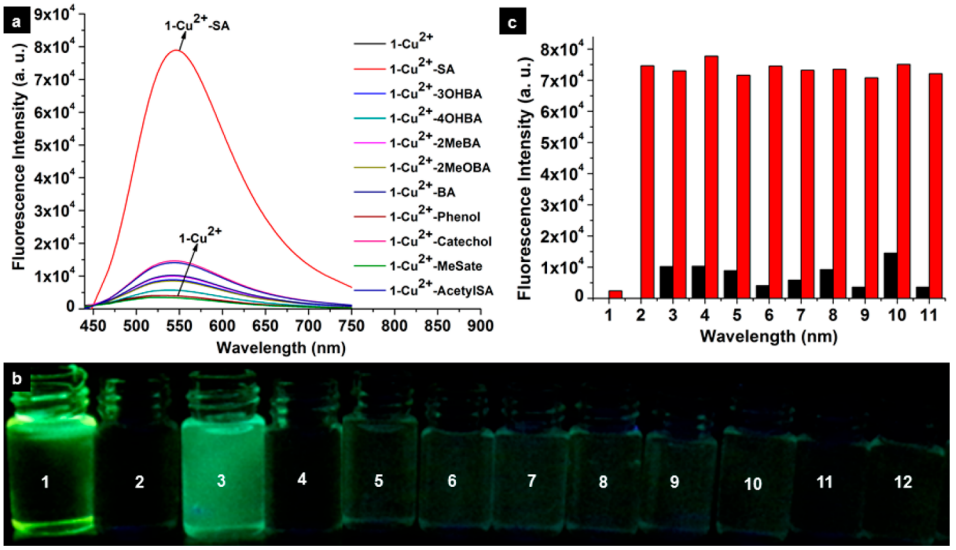

Figure 3. (a) Fluorescent spectra of **1**−Cu^{2+} (10 μM) toward 20 equiv of salicylic acid or its analogues in DMF/H_2O (7:3, v/v) ($\lambda_{ex}/\lambda_{em}$ = 433 nm/530 nm, slits = 3 nm/3 nm). (b) Photographs of **1** (10 μM), **1**−Cu^{2+} ensemble, and **1**−Cu^{2+} ensemble after the addition of 20 equiv of SA and its analogues: (1) **1**, (2) **1** + Cu^{2+}, (3) **1** + Cu^{2+} + SA, (4) **1** + Cu^{2+} + BA, (5) **1** + Cu^{2+} + 3-OHBA, (6) **1** + Cu^{2+} + 4-OHBA, (7) **1** + Cu^{2+} + 2-MeOBA, (8) **1** + Cu^{2+} + 2-MeBA, (9) **1** + Cu^{2+} + MeSate, (10) **1** + Cu^{2+} + Catechol, (11) **1** + Cu^{2+} + Phenol, and (12) **1** + Cu^{2+} + AcetylSA in DMF/H_2O (7:3, v/v) under a UV lamp with an excitation of 365 nm. (c) Competition experiments for adding SA (red bars, 20 equiv, 3−11) into the premixed solution consisting of **1**−Cu^{2+} (10 μM) and various interfering SA analogues (blank bars, 20 equiv, 3−11): (1) **1**−Cu^{2+}, (2) SA, (3) 2-CH_3BA, (4) catechol, (5) BA, (6) phenol, (7) 2-MeOBA, (8) 3-OHBA, (9) 4-OHBA, (10) AcetylSA, and (11) MeSate.

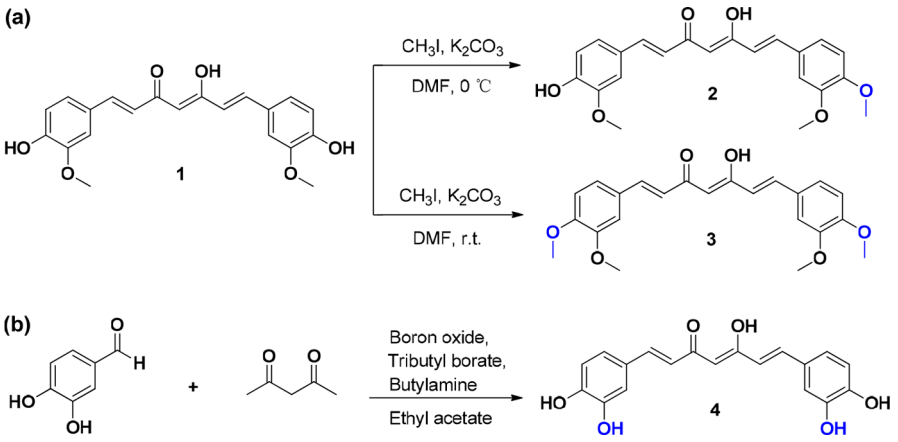

Figure 4. (a) Synthesis of probes **2** and **3**. (b) Synthesis of probe **4**.

3.3. Preparation of Curcumin Derivatives 2, 3, and 4 for Detecting SA by Their Related Cu^{2+} Ensembles. In order to explore and search for better-performance probes for monitoring SA, curcumin derivatives **2** and **3** were first designed and synthesized by the partial or complete methylation reactions on probe **1** (Figure 4 and Figures S11−S16). Undesirably, the two probes exerted a weaker selectivity for SA detection (Figures S17 and S18), indicating that the free hydroxyl groups on the benzene rings may serve as one of the critical roles in specifically distinguishing SA. Therefore, compound **4**, bearing four hydroxyl groups, was subsequently prepared (Figures S19−S21). Although probe **4** demonstrated a better selective detection capability toward SA than those of compounds **2** and **3**, it only resulted in an approximately 6-fold fluorescence enhancement at 550 nm (Figure S22), further confirming that the natural framework curcumin can be regarded as a considerable colorimetric probe for detecting SA with the privileged performance.

3.4. Possible Detection Mechanism Investigations. The ^{1}H NMR titration experiments were conducted to understand the possible mechanism and the natural interactions of **1**−Cu^{2+} and **1**−Cu^{2+}−SA. Upon addition of 1.0 equiv of Cu^{2+} to **1** (Figure 5a), the protons located at the benzene ring and olefin of **1** shifted upfield and became broadened due to the paramagnetic nature and shielding effect of Cu^{2+} (Figure 5b). Followed by the addition of 1.0 equiv of SA into the system, all of the protons belonging to SA shifted upfield due to the formation of new coordination bonds between copper ions and SA, suggesting a ternary complex **1**−Cu^{2+}−SA might be fabricated (Figure 5c,d), which was confirmed by the result from the HRMS spectrum, which provided the peak at m/z 566.4279, corresponding to the ternary complex [**1**−Cu^{2+}−SA] (Figure S23). Further study revealed that there were negligible interactions between probe **1** and SA (Figures S24 and S25). Another way titration experiments were carried out was by the addition of probe **1** into the premixed solution of SA and Cu^{2+} (Figure 5e,f). A

https://dx.doi.org/10.1021/acs.jafc.0c01283
J. Agric. Food Chem. XXXX, XXX, XXX−XXX

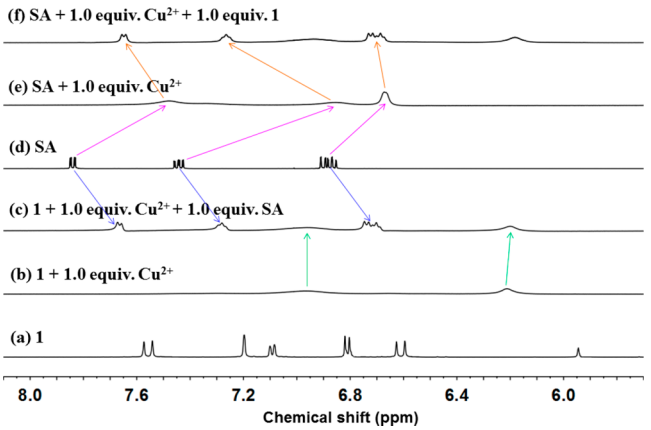

Figure 5. Partial ^{1}H NMR titration experiments of SA toward **1**−Cu^{2+} and of **1** toward SA−Cu^{2+} in CD_3OD: (a) **1**, (b) **1** + 1.0 equiv of Cu^{2+}, (c) **1**−Cu^{2+} + 1.0 equiv of SA, (d) SA, (e) SA + 1.0 equiv of Cu^{2+}, and (f) SA−Cu^{2+} + 1.0 equiv of **1**.

phenomenon was observed that the protons of SA shifted low field, which might be explained by the decreased shielding effect caused by the newly involved coordination bonding forces between probe **1** and Cu^{2+}, suggesting that Cu^{2+}, as a mediate bridge, plays the significant role in the detection of SA. The above results validated our proposed mechanism (Figure 1a).

3.5. Fluorescence Imaging. Because probe **1**−Cu^{2+} displays promising applications in monitoring SA, NRK-52E cells were used for SA imaging. Briefly, NRK-52E cells were incubated with 30 μM probe **1** for 1 h at 37 °C and then washed with 0.01 M PBS buffer (pH 7.4) thrice before imaging. A considerable fluorescence was presented for tested cells in Figure 6a, indicating that probe **1** had a good ability to penetrate the cell membrane. Cells were then incubated with culture medium containing 60 μM Cu^{2+} for another 2 h at 37 °C and then washed with 0.01 M PBS buffer thrice. Subsequently, SA-free culture medium was added into cells treated with the **1**−Cu^{2+} ensemble; no fluorescent cells were observed (Figure 6b), suggesting neither the components from the culture medium nor the ingredients inside the cell could recover the fluorescence. Finally, a strong emerging fluorescence response with different levels from the intracellular area was observed after adding different concentrations of SA for 2.5 h at 37 °C (Figure 6c,d). These results suggested that the **1**−Cu^{2+} ensemble could be used for detecting SA in living cell lines.

In conclusion, we have developed a simple, rapid, and reliable approach for detecting SA *in vitro* and *in vivo* by utilizing the natural hybrid combination of curcumin and Cu^{2+}. During the fabrication of the curcumin−Cu^{2+} ensemble, we found that Cu^{2+} could be selectively recognized by curcumin with the detection limit of 15 nM directed by a fluorescence "turn-off" mode. By introducing SA into the prepared curcumin−Cu^{2+} ensemble, the fluorescence "turn-on" pattern

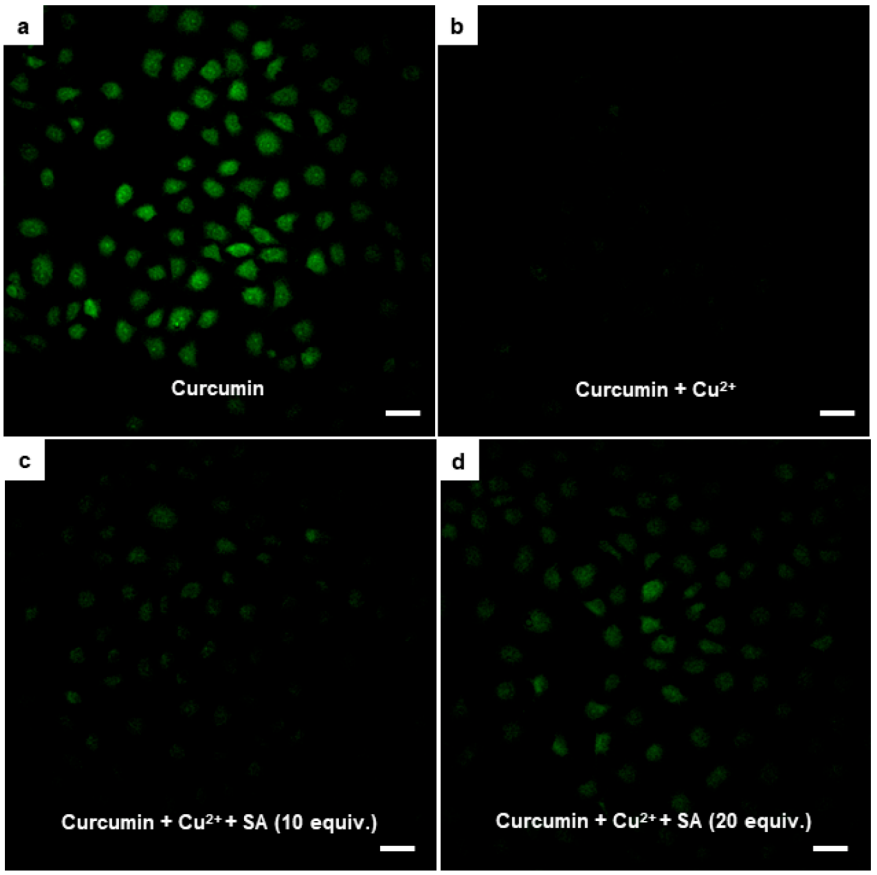

Figure 6. Confocal fluorescence microscopic images of NRK-52E cell lines under different conditions: (a) **1**, (b) **1** + Cu^{2+}, (c) **1** + Cu^{2+} + SA (10.0 equiv), and (d) **1** + Cu^{2+} + SA (20.0 equiv). The samples were washed with PBS buffer (0.01 M, pH 7.4) three times before imaging. λ_{ex} = 885 nm (two-photon excited mode), and scale bars are 40 μm.

https://dx.doi.org/10.1021/acs.jafc.0c01283
J. Agric. Food Chem. XXXX, XXX, XXX−XXX

was observed with high selectivity, providing the detection limit of 3 μM. Further study revealed that the rationally designed **1**−Cu^{2+} ensemble could sense SA in cell lines. Considering the simple, natural structure and conveniently prepared protocols for the ensemble, we anticipate that this finding can initiate the discovery of a high-performance SA probe.

■ ASSOCIATED CONTENT

Supporting Information

The Supporting Information is available free of charge at https://pubs.acs.org/doi/10.1021/acs.jafc.0c01283.

Supplementary data, Job's plot experiment, titration profiles, HRMS spectrum, calculation of detection limit, solvent selection for the detection of SA, calculation of fluorescence quantum yields, fluorescence studies, pH influences, ^{1}H NMR, ^{13}C NMR and HRMS spectra, selectivities of ensembles, HRMS spectrum, and comparison of the limit of detection (PDF)

■ AUTHOR INFORMATION

Corresponding Authors

Pei-Yi Wang − *State Key Laboratory Breeding Base of Green Pesticide and Agricultural Bioengineering, Key Laboratory of Green Pesticide and Agricultural Bioengineering, Ministry of Education, Center for R&D of Fine Chemicals of Guizhou University, Guiyang 550025, China;* orcid.org/0000-0002-9904-0664; Email: pywang888@126.com

Song Yang − *State Key Laboratory Breeding Base of Green Pesticide and Agricultural Bioengineering, Key Laboratory of Green Pesticide and Agricultural Bioengineering, Ministry of Education, Center for R&D of Fine Chemicals of Guizhou University, Guiyang 550025, China; College of Pharmacy, East China University of Science & Technology, Shanghai 200237, China;* orcid.org/0000-0003-1301-3030; Email: jhzx.msm@gmail.com

Authors

Chong Chen − *State Key Laboratory Breeding Base of Green Pesticide and Agricultural Bioengineering, Key Laboratory of Green Pesticide and Agricultural Bioengineering, Ministry of Education, Center for R&D of Fine Chemicals of Guizhou University, Guiyang 550025, China*

Lin-Lin Yang − *State Key Laboratory Breeding Base of Green Pesticide and Agricultural Bioengineering, Key Laboratory of Green Pesticide and Agricultural Bioengineering, Ministry of Education, Center for R&D of Fine Chemicals of Guizhou University, Guiyang 550025, China*

A-Ling Tang − *State Key Laboratory Breeding Base of Green Pesticide and Agricultural Bioengineering, Key Laboratory of Green Pesticide and Agricultural Bioengineering, Ministry of Education, Center for R&D of Fine Chemicals of Guizhou University, Guiyang 550025, China*

Rong Dong − *State Key Laboratory Breeding Base of Green Pesticide and Agricultural Bioengineering, Key Laboratory of Green Pesticide and Agricultural Bioengineering, Ministry of Education, Center for R&D of Fine Chemicals of Guizhou University, Guiyang 550025, China*

Zhi-Bing Wu − *State Key Laboratory Breeding Base of Green Pesticide and Agricultural Bioengineering, Key Laboratory of Green Pesticide and Agricultural Bioengineering, Ministry of Education, Center for R&D of Fine Chemicals of Guizhou University, Guiyang 550025, China*

Zhong Li − *College of Pharmacy, East China University of Science & Technology, Shanghai 200237, China*

Complete contact information is available at: https://pubs.acs.org/10.1021/acs.jafc.0c01283

Author Contributions

#C.C. and L.-L.Y. contributed equally to this work.

Notes

The authors declare no competing financial interest.

■ ACKNOWLEDGMENTS

We acknowledge the National Natural Science Foundation of China (21877021, 21702037, 31860516, 21662009), the Research Project of Ministry of Education of China (20135201110005, 213033A), and the Guizhou Provincial S&T Program (LH [2017]7259, [2017]5788).

■ REFERENCES

(1) Fu, Z. Q.; Yan, S.; Saleh, A.; Wang, W.; Ruble, J.; Oka, N.; Mohan, R.; Spoel, S. H.; Tada, Y.; Zheng, N.; Dong, X. NPR3 and NPR4 are receptors for the immune signal salicylic acid in plants. *Nature* **2012**, *486*, 228−232.

(2) Gust, A. A.; Nürnberger, T. Plant immunology: A life or death switch. *Nature* **2012**, *486*, 198−199.

(3) Kachroo, A.; Robin, G. P. Systemic signaling during plant defense. *Curr. Opin. Plant Biol.* **2013**, *16*, 527−533.

(4) Pieterse, C. M.; Van der Does, D.; Zamioudis, C.; Leon-Reyes, A.; Van Wees, S. C. Hormonal modulation of plant immunity. *Annu. Rev. Cell Dev. Biol.* **2012**, *28*, 489−521.

(5) Vlot, A. C.; Dempsey, D. M. A.; Klessig, D. F. Salicylic acid, a multifaceted hormone to combat disease. *Annu. Rev. Phytopathol.* **2009**, *47*, 177−206.

(6) Durrant, W. E.; Dong, X. Systemic acquired resistance. *Annu. Rev. Phytopathol.* **2004**, *42*, 185−209.

(7) Kachroo, A.; Robin, G. P. Systemic signaling during plant defense. *Curr. Opin. Plant Biol.* **2013**, *16*, 527−533.

(8) Dempsey, D'M. A.; Klessig, D. F. SOS - too many signals for systemic acquired resistance? *Trends Plant Sci.* **2012**, *17*, 538−545.

(9) Metraux, J. P.; Signer, H.; Ryals, J.; Ward, E.; Wyss-Benz, M.; Gaudin, J.; Raschdorf, K.; Schmid, E.; Blum, W.; Inverardi, B. Increase in salicylic acid at the onset of systemic acquired resistance in cucumber. *Science* **1990**, *250*, 1004−1006.

(10) Durner, J.; Shah, J.; Klessig, D. F. Salicylic acid and disease resistance in plants. *Trends Plant Sci.* **1997**, *2*, 266−274.

(11) Spoel, S. H.; Dong, X. How do plants achieve immunity? Defence without specialized immune cells. *Nat. Rev. Immunol.* **2012**, *12*, 89−100.

(12) Pandith, A.; Hazra, G.; Kim, H. S. A new fluorogenic sensing platform for salicylic acid derivatives based on pi-pi and NH-pi interactions between electron -deficient and electron-rich aromatics. *Spectrochim. Acta, Part A* **2017**, *178*, 151−159.

(13) Kumar, A.; Lee, J. Y.; Kim, H. S. Selective fluorescence sensing of 3,5-dinitrosalicylic acid based on pyrenesulfonamide-functionalized inorganic/organic hybrid nanoparticles. *J. Ind. Eng. Chem.* **2016**, *44*, 82−89.

(14) Kumar, A.; Pandith, A.; Kim, H. S. Pyrenebutylamidopropy-limidazole as a multi-analyte sensor for 3,5-dinitrosalicylic acid and Hg^{2+} ions. *J. Lumin.* **2016**, *172*, 309−316.

(15) Wang, P. Y.; Luo, X.; Yang, L. L.; Zhao, Y. C.; Dong, R.; Li, Z.; Yang, S. A rhodamine-based highly specific fluorescent probe for the in situ and in vivo imaging of the biological signalling molecule salicylic acid. *Chem. Commun.* **2019**, *55*, 7691−7694.

(16) Gupta, V. D. Quantitative determination of benzoic acid and salicylic acid in ointments by high-pressure liquid chromatography. *J. Pharm. Sci.* **1977**, *66*, 110−111.
(17) Siebert, D. M.; Bochner, F. Determination of plasma aspirin and salicylic acid concentrations after low aspirin doses by high-performance liquid chromatography with post-column hydrolysis and fluorescence detection. *J. Chromatogr., Biomed. Appl.* **1987**, *420*, 425−431.
(18) Venema, D. P.; Hollman, P. C. H.; Janssen, K. P.; Katan, M. B. Determination of acetylsalicylic acid and salicylic acid in foods, using HPLC with fluorescence detection. *J. Agric. Food Chem.* **1996**, *44*, 1762−1767.
(19) Aboul-Soud, M. A. M.; Cook, K.; Loake, G. J. Measurement of salicylic acid by a high-performance liquid chromatography procedure based on ion-exchange. *Chromatographia* **2004**, *59*, 129−133.
(20) Watson, J. R.; Crescuolo, P.; Matsui, F. Rapid simultaneous determination of salicylic acid and aspirin by GC I: Analysis of synthetic aspirin-salicylic acid mixtures and of single-component aspirin tablets. *J. Pharm. Sci.* **1971**, *60*, 454−458.
(21) Tanchev, S.; Ioncheva, N.; Genov, N.; Malchev, E. Gas chromatographic identification of phenolic acids found in sweet cherry and sour cherry juice. *Nahrung* **1980**, *24*, 251−253.
(22) Gupta, V. D. Quantitative determination of salicylic acid and benzoic acid in ointments. *J. Pharm. Sci.* **1972**, *61*, 1625−1626.
(23) Salinas, F.; de la Peña, A. M.; Durán-Merás, I.; Durán, M. S. Determination of salicylic acid and its metabolites in urine by derivative synchronous spectrofluorimetry. *Analyst* **1990**, *115*, 1007−1011.
(24) Adams, S.; Miller, J. M. B. The determination of salicylic acid and benzoic acid in pharmaceutical formulations by spectrofluorimetry. *J. Pharm. Pharmacol.* **1978**, *30*, 81−83.
(25) Robertson, G. L.; Kermode, W. J. Salicylic acid in fresh and canned fruit and vegetables. *J. Sci. Food Agric.* **1981**, *32*, 833−836.
(26) Tian, M.; von Dahl, C. C.; Liu, P. P.; Friso, G.; van Wijk, K. J.; Klessig, D. F. The combined use of photoaffinity labeling and surface plasmon resonance-based technology identifies multiple salicylic acid-binding proteins. *Plant J.* **2012**, *72*, 1027−1038.
(27) Fung, Y. S.; Luk, S. F. Determination of salicylic acid in pharmaceutical formulations and foods by differential-pulse voltammetry using a glassy carbon electrode. *Analyst* **1989**, *114*, 943−945.
(28) Sun, L.-J.; Feng, Q.-M.; Yan, Y.-F.; Pan, Z.-Q.; Li, X.-H.; Song, F.-M.; Yang, H.; Xu, J.-J.; Bao, N.; Gu, H.-Y. Paper-based electroanalytical devices for *in situ* determination of salicylic acid in living tomato leaves. *Biosens. Bioelectron.* **2014**, *60*, 154−160.
(29) Mahapatra, A. K.; Mondal, S.; Manna, S. K.; Maiti, K.; Maji, R.; Uddin, M. R.; Mandal, S.; Sarkar, D.; Mondal, T. K.; Maiti, D. K. A new selective chromogenic and turn-on fluorogenic probe for copper (II) in solution and Vero cells: recognition of sulphide by [CuL]. *Dalton Trans.* **2015**, *44*, 6490−6501.
(30) Fang, Y.; Chen, W.; Shi, W.; Li, H.; Xian, M.; Ma, H. A near-infrared fluorescence off−on probe for sensitive imaging of hydrogen polysulfides in living cells and mice *in vivo*. *Chem. Commun.* **2017**, *53*, 8759−8762.
(31) Li, H. D.; Yao, Q. C.; Fan, J. L.; Jiang, N.; Wang, J. Y.; Xia, J.; Peng, X. J. A fluorescent probe for H_2S *in vivo* with fast response and high sensitivity. *Chem. Commun.* **2015**, *51*, 16225−16228.
(32) Shi, B.; Gu, X.; Wang, Z.; Xu, G.; Fei, Q.; Tang, J.; Zhao, C. Fine regulation of porous architectures of core-shell silica nanocomposites offers robust nanoprobes with accelerated responsiveness. *ACS Appl. Mater. Interfaces* **2017**, *9*, 35588−35596.
(33) Zhu, L.; Xu, J.; Sun, Z.; Fu, B.; Qin, C.; Zeng, L.; Hu, X. A twisted intramolecular charge transfer probe for rapid and specific detection of trace biological SO_2 derivatives and bio-imaging applications. *Chem. Commun.* **2015**, *51*, 1154−1156.
(34) Zhang, B.; Yang, X.; Zhang, R.; Liu, Y.; Ren, X.; Xian, M.; Ye, Y.; Zhao, Y. Lysosomal-targeted two-photon fluorescent probe to sense hypochlorous acid in live cells. *Anal. Chem.* **2017**, *89*, 10384−10390.
(35) Guo, Q.; Liu, Y.; Jia, Q.; Zhang, G.; Fan, H.; Liu, L.; Zhou, J. Ultrahigh sensitivity multifunctional nanoprobe for the detection of hydroxyl radical and evaluation of heavy metal induced oxidative stress in live hepatocyte. *Anal. Chem.* **2017**, *89*, 4986−4993.
(36) Shi, H.; Kwok, R. T.; Liu, J.; Xing, B.; Tang, B. Z.; Liu, B. Real-time monitoring of cell apoptosis and drug screening using fluorescent light-up probe with aggregation-induced emission characteristics. *J. Am. Chem. Soc.* **2012**, *134*, 17972−17981.
(37) Venkatesh, Y.; Das, J.; Chaudhuri, A.; Karmakar, A.; Maiti, T. K.; Singh, N. D. P. Light triggered uncaging of hydrogen sulfide (H_2S) with real-time monitoring. *Chem. Commun.* **2018**, *54*, 3106−3109.
(38) Santos-Figueroa, L. E.; Moragues, M. E.; Climent, E.; Agostini, A.; Martínez-Máñez, R.; Sancenón, F. Chromogenic and fluorogenic chemosensors and reagents for anions. A comprehensive review of the years 2010−2011. *Chem. Soc. Rev.* **2013**, *42*, 3489−3613.
(39) Lintvedt, R. L.; Russell, H. D.; Holtzclaw, H. F., Jr Polarographic reduction of copper chelates of 1,3-diketones. IV. chelate stability and electron-transfer mechanism. *Inorg. Chem.* **1966**, *5*, 1603−1607.
(40) Hendrickson, A. R.; Martin, R. L. Thio derivatives of 1,3-diketones and their metal complexes. *O*-Ethyl thioacetothioacetato complexes of tervalent Group VIII metals. *Inorg. Chem.* **1975**, *14*, 979−982.
(41) Goan, J. C.; Huether, C. H.; Podall, H. E. The photochemical reaction of metal carbonyls with 1,3-diketones. *Inorg. Chem.* **1963**, *2*, 1078−1079.
(42) Wu, Y.; Zhang, D.; Chu, J. Y.; Boyle, P.; Wang, Y.; Brindle, I. D.; De Luca, V.; Despres, C. The *Arabidopsis* NPR1 protein is a receptor for the plant defense hormone salicylic acid. *Cell Rep.* **2012**, *1*, 639−647.
(43) Palanisami, N.; Prabusankar, G.; Murugavel, R. A novel dimeric copper salicylate with an undissociated COOH group: Synthesis and crystal structure of $[Cu_2(HSal)(Sal)(2,20\text{-bpy})_2](ClO_4)$. *Inorg. Chem. Commun.* **2006**, *9*, 1002−1006.
(44) O'Connor, M.; Kellett, A.; McCann, M.; Rosair, G.; McNamara, M.; Howe, O.; Creaven, B. S.; McClean, S.; Foltyn-Arfa Kia, A.; O'Shea, D.; Devereux, M. Copper(II) complexes of salicylic acid combining superoxide dismutase mimetic properties with DNA binding and cleaving capabilities display promising chemotherapeutic potential with fast acting in vitro cytotoxicity against cisplatin sensitive and resistant cancer cell lines. *J. Med. Chem.* **2012**, *55*, 1957−1968.
(45) Sharma, J.; Singh, A.; Sharma, R.; Singh, Y.; Vir Singh Teotia, U. Synthesis and antioxidant appraisal of curcumin and two curcuminoid compounds. *Der Pharm. Sin.* **2013**, *4*, 151−163.

https://dx.doi.org/10.1021/acs.jafc.0c01283
J. Agric. Food Chem. XXXX, XXX, XXX−XXX